Originalarbeit

BHM (2017) Vol. 162 (8): 319–325
DOI 10.1007/s00501-017-0638-z

BHM Berg- und Hüttenmännische Monatshefte

Comparative Laboratory Studies of Conventional and Electrodynamic Fragmentation of an Industrial Mineral

Julia Tschugg, Wolfgang Öfner, and Helmut Flachberger

Chair of Mineral Processing, Department Mineral Resources Engineering, Montanuniversität Leoben, Leoben, Austria

Received July 3, 2017; accepted July 3, 2017; published online July 26, 2017

Abstract: In order to address comminution efficiency, which could be defined as the increase in mass specific surface against net specific energy input, the energy consumption of an industrial mineral with and without pre-weakening by high voltage pulses covering the same size range were compared. The three tested comminution sequences consisted of a laboratory jaw crusher or pilot scale high voltage pulse machine at two different circulating loads, a laboratory crusher and two tumbling mills of differing grinding media; all being operated following the principles of energy optimized comminution according to the OCS-method. The first results indicate that possible energy reduction by electrodynamic pre-weakening is available in the immediately subsequent, but not in further conventional comminution stages for the tested industrial mineral.

Keywords: Electrodynamic comminution, Pre-weakening, High voltage pulses, Mineral processing, Industrial minerals, Optimized Comminution Sequence

Vergleichende aufbereitungstechnische Laboruntersuchungen von konventioneller Zerkleinerung und elektrodynamischer Fragmentierung eines Industrieminerals

Zusammenfassung: Um die Effizienz eines Zerkleinerungsprozesses, bei welchem der massenspezifische Oberflächenzuwachs einem Nettoenergieeintrag gegenübergestellt wird, zu beurteilen, wurde der Energieverbrauch mit und ohne Vorschwächung durch Hochspannungsimpulsbehandlung gleicher Korngrößenfraktionen an einem Industriemineral gegenübergestellt. Die Zerkleinerungskette bestand aus einem Laborbackenbrecher bzw. einer Pilotanlage zur Behandlung mit Hochspannungsimpulsen, einem Laborbackenbrecher und zwei Trommelmühlen, die dem Prinzip der energieoptimierten Zerkleinerung gemäß der OZK-Methode folgten. Erste Ergebnisse mit dem verwendeten Industriemineral zeigen auf, dass ein Energieeinsparungspotential bedingt durch elektrodynamische Vorschwächung in der unmittelbar darauffolgenden, aber nicht in weiter entfernten Zerkleinerungsstufen erkennbar ist.

Schlüsselwörter: Elektrodynamische Zerkleinerung, Vorschwächung, Hochspannungsimpulse, Aufbereitung und Veredlung, Industrieminerale, Optimierte Zerkleinerungskette

1. Introduction

Comminution remains by far the largest energy consumer in mineral processing implying high operational costs and a big greenhouse footprint. One potential method to reduce the energy consumption of comminution might be pre-weakening by high voltage pulses as shown in prior studies on different raw materials in mineral processing [1–4].

Electrodynamic breakage inside particles that are immersed in water and positioned between two electrodes is initiated by high voltage pulses, which disintegrate and/or weaken the particles' structure by strong tensile forces due to the differences in mechanical or electrical properties of different components [5–8]. Significant reductions of ore particle strength were visible after the application of high voltage pulses of low specific energy [2] and have demonstrated the potential to decrease the energy consumption in the downstream comminution process, especially in hybrid circuit simulations [9].

Pre-weakening after the application of a single high voltage pulse was for the first time described as "softening" of an emerald-bearing pegmatite matrix [10]. Further studies

Dipl.-Ing. J. Tschugg (✉)
Chair of Mineral Processing, Department Mineral Resources Engineering,
Montanuniversität Leoben,
Franz-Josef-Straße 18,
8700 Leoben, Austria
julia.tschugg@unileoben.ac.at

regarding electrodynamic weakening were executed with different laboratory equipment, either commercially available like the SELFRAG Lab [2, 11] or self-constructed like the High Voltage Electric Pulses Crusher built at the Iranian Amirkabir University of Technology [4]. To demonstrate the benefits of pre-weakening by high voltage pulses to the mineral industry, to treat larger particles and to use more flexible operation settings, a pilot scale Pre-Weakening Testing Station (PWTS) was developed by SELFRAG AG (SELFRAG) and used to further characterize pre-weakening by high voltage pulse treatment [3, 12].

In prior experimental work, analyses comparing the original to the residual hardness after high voltage pulse treatment included the Julius Kruttschnitt Rotary Breakage Tester, various Bond tests, mercury porosimetry and X-ray Cone Beam Tomography (CBT) to measure cracks/microcracks [2, 4, 8, 13, 14]. The present study investigates the comminution properties of an industrial mineral after a stage of conventional crushing or high voltage pulse treatment. This results in electrodynamic fragmentation and potential pre-weakening with respect to its individual breakage characteristics and the specific energy consumption as a function of the product dispersity. Other expected advantages of this comminution method like selective fragmentation to improve mineral liberation at coarse particle sizes [7, 10, 15] or pre-concentration [16, 17] are not discussed in this paper.

2. Methods, Equipment and Materials

2.1 The OCS Method

The Optimized Comminution Sequence (OCS), an extensive laboratory experimental work scheme, has been developed at the Chair of Mineral Processing, Montanuniversität Leoben [18–20], and is based on the idea of establishing a comminution process that minimizes the energy consumption Δe for a given size reduction step i. The OCS is a tool developed to characterize comminution properties of minerals and rocks regarding their individual breakage characteristics independent from the influence of machinery. The specific energy consumption is a function of product dispersity, which is described by the particle size distribution and the specific surface area of the products [21, 22].

Numerous comminution stages in closed circuit, with pre-screening at small size-reduction ratio (<1:4) and high circulating load (>100%) are the characteristics for the OCS obeying the principle of energy-optimized comminution. The adjustment of the comminution tool of each stage is optimized with regard to the feed size. Fines in the feed are separated by pre-screening, directing the energy supplied by the comminution tool to the coarse particles. Each comminution cycle ends with intermediate classification at a defined screen aperture to remove the fine particles swiftly after their creation. This short retention time of the particles results in a smaller number of stress events per particle and cycle. Additionally, this leads to a material specific particle size distribution and minimum energy dissipation by compaction. The net energy consumption and the specific surface area of selected particle size classes of the comminution product are measured at each stage, as well as the particle size distribution of the feed and the comminution product [18, 21, 23].

When brittle mineral matter is fragmented in subsequent sub-circuits of small size reduction ratio, known as OCS, this results in the steepest possible cumulative fragmentation due to the lowest amount of fines, and minimum variation of particle sizes (and specific surfaces) possible at this particular maximum particle size. This is one aspect of the Natural Breakage Characteristics (NBC). After further comminution steps, the resulting fragmentation sieving curves plotted on a GGS-grid (Gates, Gaudin and Schuhmann plot) are shifted vertically upwards in a full logarithmic diagram, indicating self-similarity of the comminution progress. This implies that the local slope of the curve depends only on the "pure" fragmentation itself and is independent of equipment and processing [18, 20].

The cumulative display of the particle size distribution in the full logarithmic GGS-grid allows the distinction between homogeneous and inhomogeneous raw material behaviour by the degree of linearization of the distribution [18]. Particle size distributions of OCS products of inhomogeneous materials do not follow any power function, but the local uniformity factor (GGS exponent) remains largely independent from the maximum particle size. For homogeneous raw materials there is a linearization and ideally one single uniformity coefficient characterizes the total distribution over all maximum particle sizes. The particle size distributions from OCS are parallel to each other in the GGS-grid independent of raw material behaviour [22].

For an optimal sequence of fragmentation steps, a gain in mass specific surface (Δa, cm^2/g), determined by permeametry, and specific energy consumption (Δe, J/g) are linearly dependent (down to a k_{max} of 40 µm). The slope represents a parameter of the rock, characterizing the natural fragmentation behaviour of the raw material, and its gradient is the Rittinger coefficient of comminution (R, cm^2/J). According to [24], the Rittinger coefficient covers roughly a range between 10 cm^2/J for low grindability samples (e. g. thermally compacted slags) and 150 cm^2/J (e. g. unconsolidated limestone) [20, 25].

$$\Delta a = R \cdot \Delta e \tag{1}$$

A complete characterization of the comminution behaviour of a given raw material is possible by the Rittinger coefficient, the uniformity coefficient, a raw material related shape factor and the nominal minimum particle size [23, 24].

2.2 Test Procedure

Three Optimized Comminution Sequences are compared in this investigation. They consist of either one crushing (jaw crusher 1) or one electrodynamic stage (PWTS 100% or PWTS 250%), another crushing stage (jaw crusher 2) and finally two grinding stages (rod mill and ball mill) as demon-

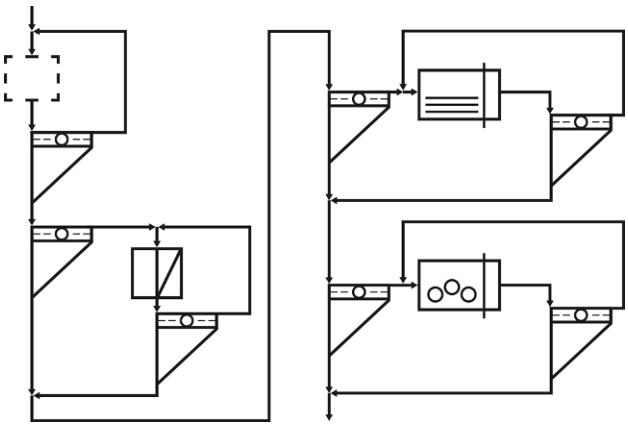

Fig. 1: Flow sheet of the OCS set-up for the current investigation – the dashed square is a placeholder for either the jaw crusher 1 or the PWTS with circulating loads of 100% or 250%

strated in Fig. 1. The different maximum feed size, split cut and circulating load of all stages are shown in Table 1. The circulating load given for comminution stage 1 is 100% for conventional comminution by jaw crusher 1. For the fragmentation and pre-weakening by high voltage pulses, in one sequence the circulating load was 100% (PWTS 100%), in the other 250% (PWTS 250%).

After each fragmentation step the comminution product was sieved manually, the oversize was topped up with fresh feed and recycled to the fragmentation unit, and the undersize was dried if necessary and stored for analysis. For the determination of particle size distribution, specific surface and energy consumption, either the mean was calculated from the three cycles in steady state for jaw crusher and mills, or representative samples were taken from steady state electrodynamic fragmentation. All the particle size distributions received from manual sieving were corrected by the results of air-jet sieving at 40 µm prior to the data evaluation and analysis.

2.3 Jaw Crusher

The laboratory jaw crusher BB 200 by Retsch was used at the first stage (Jaw crusher 1 for the conventional comminution sequence only) and for the second comminution step during the OCS (Jaw crusher 2 for the conventional and both sets of high voltage treated process lines). The gap width was set to obtain the required product at a specific circulating load as given in Table 1. To measure and record the true power consumption in a standard electric circuit with symmetric load, a digital multimeter (VOLTCRAFT M-4660M) connected to a PC by a RS 232-interface was used. The mean net energy consumption resulted from the total power draw reduced by the mean idle power draw measured before and after crushing, and the duration of the actual crushing action [23].

2.4 Pre-Weakening Testing Station (PWTS)

The electrodynamic fragmentation (and pre-weakening) by high voltage pulses was done with a pilot scale PWTS machine installed at SELFRAG in Kerzers, Switzerland. The PWTS unit presented in Fig. 2 comprises a pulse generator, a metal plate conveyor, a water vessel and a processing zone (Fig. 3). The immersed sample is processed between a disk-shaped top electrode which is connected to the pulse generator, and the flat bottom section of the metal plate conveyor acting as counter electrode. Adjustable parameter settings of the PWTS are voltage (50–200 kV), pulse energy (27.5–750.0 J), electrode gap (10–80 mm, which limits the maximum feed particle size), polarity (positive or negative), frequency (1–100 Hz), operation mode (batch with stationary or continuous with moving conveyor) and throughput (0–10 t/h). The installed power is 20 kW. The operational settings of the experimental work for PWTS 100% and PWTS 250% are shown in Table 2. The flexible generator setup with adjustable voltage and capacitance allows the testing with the same pulse energy, but at different voltages [12].

The used generator energy can be calculated for the PWTS from given parameter settings. It relates to the power taken from the power grid and refers to overall energy consumption, being a function of total capacitance of all capacitors used in the generator, the charging voltage supplied to the circuit, and the number of pulses applied. However, to date it is not possible to calculate or measure its actual spark energy like for the SELFRAG Lab, which is a laboratory unit of the same manufacturer. As the net fragmentation energy of the PWTS is not available, it is omitted at the first stage of all three comminution sequences. Instead, the focus is set to evaluate possible pre-weakening in subsequent fragmentation steps.

2.5 Tumbling Mills

For the third comminution stage a rod mill, and for the fourth stage a ball mill were used. The dimensions and settings of both laboratory mills are given in Table 3 and are illustrated in detail in [22].

TABLE 1
Maximum feed size, split cut and circulating load for comminution stages 1 to 4

Comminution stage	Max. feed size (mm)	Split cut (mm)	Circulating load (%)
1	40.0	20.0	100 or 250
2	20.0	6.3	100
3	6.3	1.0	100
4	1.0	0.2	250

Fig. 2: Illustration of the PWTS

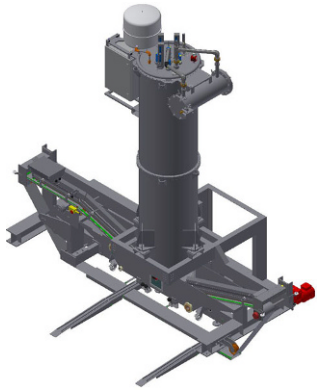

Fig. 3: Processing zone of the PWTS showing the pulse generator, the disk-shaped top electrode, the counter electrode (metal plate conveyor) and the insulation material for side guides

TABLE 2
Operational parameters of the PWTS for electrodynamic fragmentation and pre-weakening

Operational parameter	OCS comminution stage 1 (pre-weakening)	
	PWTS 100%	PWTS 250%
Gap width (mm)	50	50
Frequency (Hz)	15.0	7.7
Voltage (kV)	180	180
Capacitance (nF)	90	90
Belt speed (mm/s)	111	184
Circulating load (%)	100	250

According to [19] there is, based on the principle of similarity, a relationship between the mass specific energy input for the dispersity step of rod mill (e_m, J/g), the inner diameter of the mill (d_i, m), the mass of grinding media (m_m, g), the fines generated (m_f, g), number of revolutions (n, 1), and gravity (g, m/s^2) [22].

$$e_m = c_P \cdot g \cdot m_m \cdot d_i \cdot \frac{n}{m_f} \quad (2)$$

The dimensionless power conversion factor (or Steiner factor) c_p (1) for the mechanical power transferred into the grinding chamber was derived presuming a constant geometric and kinematic similarity and it is distributed in the range of 0.8–1.3 as determined from calibration measurements (laser aberration measurement) [19]. Bulk volume fraction of and friction conditions within the mill charge inside the mill chamber, the boundary between the charge and the shell of the tumbling mill and the ratio of centrifugal acceleration at the perimeter of the mill are expected to be rather constant [21].

Low differences between idle and load state, fluctuating voltage in the power grid and time-dependent changes in bearings and gears complicate the recording of electrical performance over time for a laboratory ball mill. An alternative approach is the measurement of the torque of the mill shaft using either a torquemeter with strain gauges, a pendulum torsion measurement, or a planetary gear. At the Chair of Mineral Processing, a torque sensor type (Hottinger Baldwin Messtechnik GmbH) with a measuring and a recording unit are used to record the energy consumption within the grinding chamber. The measuring shaft is bolted to the drive shaft between the electric motor and the mill by two rigid couplings. Four rotating strain gauges in a Wheatstone-bridge circuit are either compressed or stretched by the torque on the shaft. The measured signal is proportional to the torque. The reading in millivolt per volt of constant supply voltage is provided to a low voltage amplifier module QuantumX MX440B (HBM Inc.) which provides the time-dependent voltage signal to an electronic recording station. The software catman AP 3.4.2.52 (Hottinger Baldwin Messtechnik GmbH) allows an automatic conversion of the voltage signal into torque and calculation of its moving average [22].

The calculation of the mass specific net energy input (e_m, J/g) requires the amount of ground fines (m_f, g), the mean net torque (t_m, Nm) and the number of revolutions (n, 1) [22].

$$e_m = \frac{2\pi \cdot t_m \cdot n}{m_f} \quad (3)$$

2.6 Specific Surface Area

The evaluation of the specific surface area of all comminution products was based on permeametry. The arithmetic mean was calculated for three independent measurements of the surface with both a Blaine apparatus (by Tonindustrie Prüftechnik GmbH; constant volume) and the Permaran unit (by Outokumpu; constant pressure) for the fractions 0–40 µm and 40–100 µm [23, 25].

It can be assumed that the size classes 0–40 µm and 40–100 µm account for at least 90% of the total specific surface area of the samples and that the shape factor of the 40–100 µm fraction derived from surface equivalent particle size and the volume specific surface area of this particle size class is valid for all fractions >100 µm. Therefore it is possible to calculate their respective specific surfaces. Spe-

TABLE 3
Operational parameters of the rod mill and the ball mill

Operational parameter	OCS comminution stage 3 (rod mill)	OCS comminution stage 4 (ball mill)
Mass of grinding media (kg)	8.068	8.859
Grinding media (1)	Steel rods	Steel balls
Mill inner diameter (m)	0.15	0.20
Mill inner length (m)	0.30	0.20
Critical speed (s^{-1})	1.80	1.58
Fraction of critical speed (%)	70	70

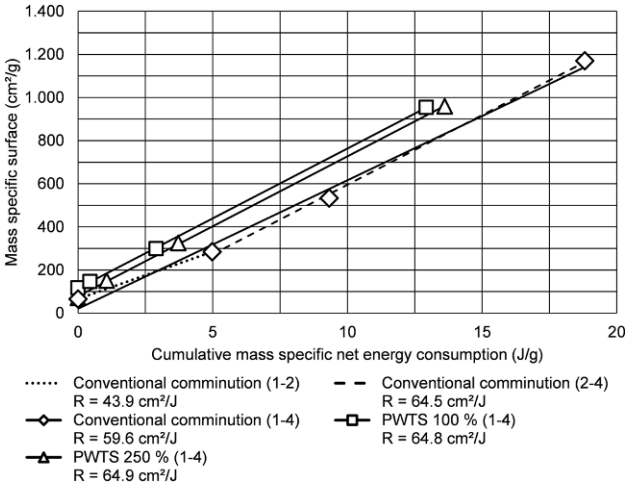

Fig. 4: Results of the cumulative mass specific energy vs. the generated mass specific surface obtained by the OCS method for conventional comminution and with electrodynamic pre-weakening (PWTS 100% and PWTS 250%)

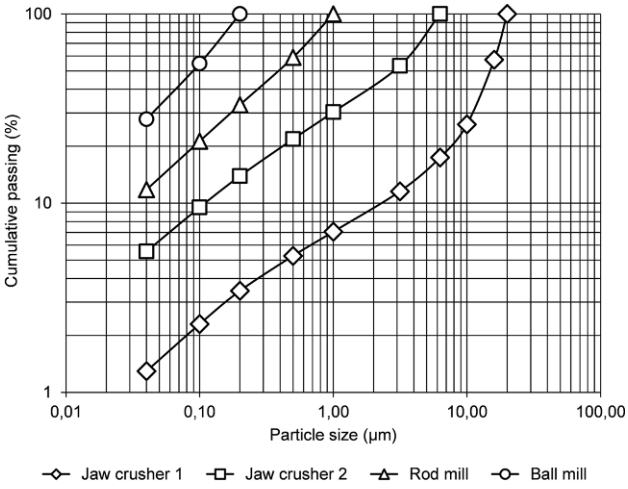

Fig. 5: Particle size distributions obtained by the OCS method for conventional comminution

cific surface area of the entire comminution product is then calculated as a weighted average [21, 25, 26].

2.7 Tested Sample

The feed was a common industrial mineral which had been crushed to 20–40 mm and washed prior to processing. Further details cannot be provided due to obligation of secrecy towards the industrial partner.

3. Results and Discussion

Fig. 4 summarizes all the results achieved from the energy and surface observations resulting from the OCS of conventional comminution and electrodynamic fragmentation at different circulating loads (100% and 250%) and allows the observation of different comminution behaviours for the two methods. As it is not possible to measure or calculate the net comminution energy of electrodynamic fragmentation performed by the Pre-Weakening Testing Station as described in Sect. 2.4, the energy input for the first fragmentation step was ignored for all three test series and only the most recently generated surface was taken into account.

Rittinger coefficients of 59.6 cm^2/J for conventional comminution, of 64.8 cm^2/J for PWTS 100% and 64.9 cm^2/J for PWTS 250% are similar to those obtained in prior studies at the Chair of Mineral Processing with feed of the same kind. Rittinger lines are nearly parallel for PWTS 100% and PWTS 250% (±0.1 cm^2/J) and reach similar values for total surface area after comminution stage 1. The slope of the entire conventional comminution sequence is a little bit lower (–5 cm^2/J). At comminution stage 1, the highest values for mass specific surface are obtained with PWTS 100% (118 cm^2/g) whereas conventional comminution and PWTS 250% are both at around 70 cm^2/g.

For jaw crusher 2, conventional comminution needed five to ten times more energy, but resulted in total surface area twice as high when operated at the same circulating load of 100%. Similar surface values for the pre-weakened raw materials are attained in the next comminution stage (rod mill).

When splitting the sequence for conventional comminution in two sections – namely from jaw crusher 1 to jaw crusher 2 and from jaw crusher 2 to ball mill, respectively – the Rittinger slope is lower only at the beginning (dotted line), 43.9 cm^2/J. For the second section (dashed line), the slope is 64.5 cm^2/J and thus becomes virtually the same as in the PWTS sequences (Fig. 4). A pre-weakening effect is thus restricted to the second jaw crusher stage in the current investigation.

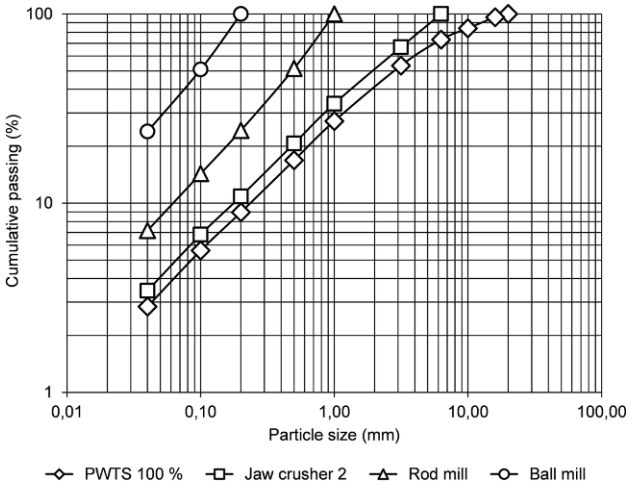

Fig. 6: Particle size distributions obtained by the OCS method with electrodynamic pre-weakening (PWTS 100%)

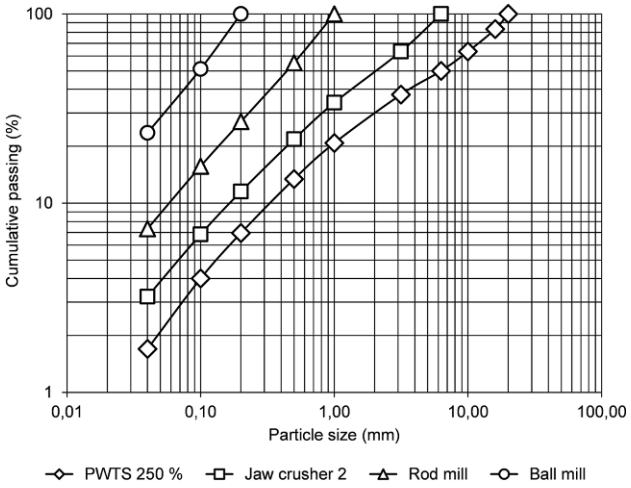

Fig. 7: Particle size distributions obtained by the OCS method with electrodynamic pre-weakening (PWTS 250%)

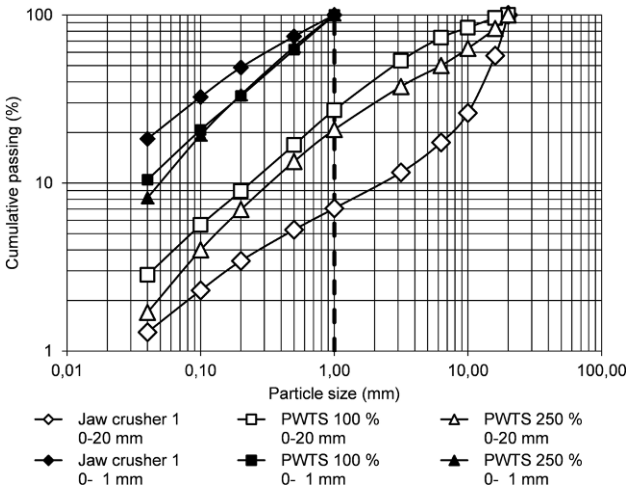

Fig. 8: Particle size distributions after the first fragmentation stage of jaw crusher 1, PWTS 100% and PWTS 250% for the observation ranges 0–20 mm and 0–1 mm

The correlation coefficient of the energy/surface relation for pre-weakening is 1.00. Strong correlation for conventional comminution (R^2 = 0.99 in the present investigation) was observed before in other OCS studies, amongst others for amphibolite and limestone [23].

The particle size distributions from sieving after the different comminution stages (Fig. 5, 6 and 7) show that while there are big differences in the first comminution stage (jaw crusher vs. electrodynamic fragmentation at different circulating loads), variations become less significant for subsequent stages. When comparing not the whole particle size range of 0–20 mm, but only particles smaller than 1 mm after the first fragmentation step, more fines <40 µm are produced during conventional comminution by jaw crusher compared to the PWTS with half the amount or less, as illustrated in Fig. 8.

4. Conclusions

Electrodynamic fragmentation has the potential to be integrated as an alternative or supportive wet comminution method into mineral processing operations. The results of recent studies undertaken at the Chair of Mineral Processing for a certain industrial mineral show that a pre-weakening effect from electrodynamic fragmentation is present only in the next fragmentation stage, but not further down the comminution sequence. An estimation of the net energy resulting from high voltage pulse treatment by PWTS is currently not possible and therefore excluded from the observation. Thus it is difficult to define the potential of the energy savings due to pre-weakening, with respect to the entire comminution chain.

The current tests confirm the lower generation of fines, as reported previously for a range of other rock types [2, 14, 27]. Less fines could increase the recovery of valuable minerals after sorting since the selectivity of separation processes is higher for coarser particle sizes, provided that selective liberation along mineral phase boundaries occurs.

Recommended further studies include the application of the electrodynamic fragmentation method especially for different industrial minerals, more intense research into potential energy savings due to pre-weakening in combined fragmentation processes, the adaptability to existing and new sorting processes characteristic for the industry, and the changes of product properties and qualities (e. g. degree of liberation) due to preferential selective fragmentation along mineral phase boundaries in coarse particle size ranges.

Acknowledgements. The financial support, the provision of raw material, equipment and intellectual input from the industrial partner is gratefully acknowledged. Furthermore, the generous offer from SELFRAG to use their facility in Kerzers and for sharing their experience and knowledge is highly appreciated.

References

1. Usov, A. F.; Tsukerman, V. A.: Electric pulse processes for processing of mineral raw materials: energy aspect, in: Önal, G.; Acarkan, N.; Çelik, M. S.; Arslan, F.; Ateşok, G.; Güney, A.; Sirkeci, A. A.; Yüce, A. E.; Perek, K. T. (Eds.): Proceedings of the XXIII International Mineral Processing Congress, XXIII International Mineral Processing Congress (IMPC 2006), Istanbul, Turkey, 2006, pp 2084–2090
2. Wang, E.; Shi, F.; Manlapig, E.: Pre-weakening of mineral ores by high voltage pulses, Minerals Engineering 24 (2011), pp 455–462
3. Van der Wielen, K. P.; Weh, A.; Hernandez, M.; Müller-Siebert, R.: A standardised methodology for the assessment of the high voltage breakage characteristics of ores, in: Minerals Engineering International: Comminution '14, Cape Town, South Africa, 2014, pp 499–520
4. Razavian, S. M.; Rezai, B.; Irannajad, M.: Investigation on pre-weakening and crushing of phosphate ore using high voltage electric pulses, Advanced Powder Technology 25 (2014), no. 6, pp 1672–1678
5. Andres, U.: Parameters of disintegration of rock by electrical pulses, Powder Technology 58 (1989), no. 4, pp 265–269
6. Andres, U.: Electrical disintegration of rock, Mineral Processing and Extractive Metallurgy Review 14 (1995), no. 2, pp 87–110
7. Andres, U.; Timoshkin, I.; Jirestig, J.; Stallknecht, H.: Liberation of valuable inclusions in ores and slags by electrical pulses, Powder Technology 114 (2001), no. 1–3, pp 40–50
8. Van der Wielen, K. P.: Application of high voltage breakage to a range of rock types of varying physical properties, Dissertation, University of Exeter, 2013
9. Shi, F.; Manlapig, E.; Zuo, W.: Progress and challenges in electrical comminution by high-voltage pulses, Chemical Engineering & Technology 37 (2014), no. 5, pp 765–769
10. Andres, U.; Bialecki, R.: Liberation of mineral constituents by high-voltage pulses, Powder Technology 48 (1986), no. 3, pp 269–277
11. Zuo, W.; Shi, F.: A t10-based method for evaluation of ore pre-weakening and energy reduction, Minerals Engineering 79 (2015), pp 212–219
12. Zuo, W.; Shi, F.; Van der Wielen, K. P.; Weh, A.: Ore particle breakage behaviour in a pilot scale high voltage pulse machine, Minerals Engineering 84 (2015), pp 64–73
13. Shi, F.; Zuo, W.; Manlapig, E.: Characterisation of pre-weakening effect on ores by high voltage electrical pulses based on single-particle tests, Minerals Engineering 50–51 (2013), pp 69–76
14. Wang, E.; Shi, F.; Manlapig, E.: Mineral liberation by high voltage pulses and conventional comminution with same specific energy levels, Minerals Engineering 27–28 (2012), pp 28–36
15. Andres, U.: Liberation study of apatite-nepheline ore comminuted by penetrating electrical discharges, International Journal of Mineral Processing 4 (1977), no. 1, pp 33–38
16. Zuo, W.; Shi, F.; Manlapig, E.: Pre-concentration of copper ores by high voltage pulses: Part 1: principle and major findings, Minerals Engineering 79 (2015), pp 306–314
17. Shi, F.; Zuo, W.; Manlapig, E.: Pre-concentration of copper ores by high voltage pulses: Part 2: opportunities and challenges, Minerals Engineering 79 (2015), pp 315–323
18. Steiner, H. J.: Rahmengesetzmäßigkeiten der natürlichen Bruchcharakteristik, Erzmetall (1990), no. 43, pp 435–440
19. Steiner, H. J.: Characterization of laboratory-scale tumbling mills, International Journal of Mineral Processing 44–45 (1996), pp 373–382
20. Steiner, H. J.: Zerkleinerungstechnische Eigenschaften von Gesteinen, Felsbau (1998), no. 16, pp 320–325
21. Niiranen, K.: Characterization of the Kiirunavaara iron ore deposit for mineral processing with a focus on the high silica ore type B2, Dissertation, Montanuniversität Leoben, 2015
22. Böhm, A.; Flachberger, H.: Überblick über Methoden der Mahlbarkeitsprüfung, BHM Berg- und Hüttenmännische Monatshefte 151 (2006), no. 6, pp 223–232
23. Böhm, A.; Mayerhofer, R.; Öfner, W.: Energy for rock breakage, Montanuniversität Leoben, https://pure.unileoben.ac.at/portal/de/publications/energy-for-rock-breakage(14a226fd-fd06-4fe3-816b-921697707b0b)/export.html (30.06.2017), 2016
24. Steiner, H. J.: The significance of the Rittinger-equation in present-day comminution technology, in: Bergakademie Freiberg: XVIIth International Mineral Processing Congress, Preprints, Volume 1, Comminution and Classification, Modelling and Process Control, Dresden, Germany, 1991, pp 177–188
25. Böhm, A.; Meissner, P.; Plochberger, T.: An energy based comparison of vertical roller mills and tumbling mills, International Journal of Mineral Processing 136 (2015), pp 37–41
26. Böhm, A.: Derivation of the specific surface area and the particle shape factor from permeametry, in: Nürnberg Messe GmbH (Ed.): Abstracts and proceedings, World Congress on Particle Technology (WCPT6), Nuremberg, Germany, 2010, pp 736–739
27. Brandt, F.; Haus, R.: New concepts for lithium minerals processing, Minerals Engineering 23 (2010), no. 8, pp 659–661

